

# Genome-wide association study of intraocular pressure uncovers new pathways to glaucoma

Stuart MacGregor<sup>1\*</sup>, Jue-Sheng Ong<sup>1</sup>, Jiyuan An<sup>1</sup>, Xikun Han<sup>1</sup>, Tiger Zhou<sup>2</sup>, Owen M. Siggs<sup>2</sup>, Matthew H. Law<sup>1</sup>, Emmanuelle Souzeau<sup>2</sup>, Shiwani Sharma<sup>2</sup>, David J. Lynn<sup>3,4,5</sup>, Jonathan Beesley<sup>1</sup>, Bronwyn Sheldrick<sup>2</sup>, Richard A. Mills<sup>2</sup>, John Landers<sup>2</sup>, Jonathan B. Ruddle<sup>6</sup>, Stuart L. Graham<sup>7</sup>, Paul R. Healey<sup>8,9</sup>, Andrew J. R. White<sup>8</sup>, Robert J. Casson<sup>10</sup>, Stephen Best<sup>11</sup>, John R Grigg<sup>9</sup>, Ivan Goldberg<sup>9</sup>, Joseph E. Powell<sup>12,13</sup>, David C. Whiteman<sup>1</sup>, Graham L. Radford-Smith<sup>1,14</sup>, Nicholas G. Martin<sup>1</sup>, Grant W. Montgomery<sup>15</sup>, Kathryn P. Burdon<sup>2,16</sup>, David A. Mackey<sup>16,17,18</sup>, Puya Gharahkhani<sup>1,18</sup>, Jamie E. Craig<sup>2,18</sup> and Alex W. Hewitt<sup>6,16,18</sup>

**Intraocular pressure (IOP) is currently the sole modifiable risk factor for primary open-angle glaucoma (POAG), one of the leading causes of blindness worldwide<sup>1</sup>. Both IOP and POAG are highly heritable<sup>2</sup>. We report a combined analysis of participants from the UK Biobank ( $n=103,914$ ) and previously published data from the International Glaucoma Genetic Consortium ( $n=29,578$ )<sup>3,4</sup> that identified 101 statistically independent genome-wide-significant SNPs for IOP, 85 of which have not been previously reported<sup>4–12</sup>. We examined these SNPs in 11,018 glaucoma cases and 126,069 controls, and 53 SNPs showed evidence of association. Gene-based tests implicated an additional 22 independent genes associated with IOP. We derived an allele score based on the IOP loci and loci influencing optic nerve head morphology. In 1,734 people with advanced glaucoma and 2,938 controls, participants in the top decile of the allele score were at increased risk (odds ratio (OR)=5.6; 95% confidence interval (CI): 4.1–7.6) of glaucoma relative to the bottom decile.**

Over the past decade, genome-wide association studies (GWAS) have implicated 14 independent loci involved in the pathogenesis of POAG<sup>4–12</sup>, and an additional eight loci have been associated with primary angle-closure glaucoma (PACG)<sup>13,14</sup>. The classification of POAG and PACG is based on the anatomical configuration of the iridocorneal angle, where outflow of aqueous humor occurs through the trabecular meshwork. Regardless of the glaucoma classification, it is well established that elevated IOP can lead to irreversible optic nerve degeneration and corresponding visual-field deficits<sup>1</sup>. Currently, all drugs used to treat glaucoma lower IOP by

either increasing aqueous outflow (through the trabecular meshwork or uveoscleral tracts) or decreasing aqueous production<sup>1</sup>. Understanding which genes influence IOP may open new avenues for glaucoma treatment. We report results from a large GWAS for IOP and glaucoma, and explore the genetic relationship between the endophenotype and the disease.

To identify SNPs influencing IOP, we undertook a meta-analysis of IOP GWAS from the publicly available UK Biobank (UKBB; see URLs) and previously published data from the International Glaucoma Genetic Consortium<sup>4</sup> (IGGC; see URLs; Supplementary Fig. 1). To determine which of the peak SNPs were statistically independent and thus potentially informative in allelic risk profiling, we used the program GCTA-COJO to perform conditional analysis on the summary meta-analysis (see URLs and Methods for full description)<sup>15</sup>. A total of 106 independent SNPs (uncorrelated with other peak SNPs) surpassed the genome-wide-significance threshold ( $P < 5 \times 10^{-8}$ ; Fig. 1, Supplementary Tables 1 and 2 and Supplementary Fig. 2). For downstream analysis, we removed five peak SNPs influencing IOP measurement through corneal biomechanics. The removed SNPs were rs66724425 in *ADAMTS6*, previously shown to be associated with central corneal thickness<sup>16</sup>, and rs1570204, rs78658973, rs12492846 and rs2797560, which were more strongly associated (i.e., had lower  $P$  values) with corneal hysteresis (a measure of viscous damping in the cornea that influences IOP measurement) than with IOP (Supplementary Table 2). Among the remaining 101 SNPs, we found strong concordance (Pearson's correlation coefficient = 0.85;  $P < 0.001$ ) in the effect sizes between IGGC and UKBB (Fig. 2a). Of the 101 associated SNPs, 85 had not

<sup>1</sup>QIMR Berghofer Medical Research Institute, Brisbane, Queensland, Australia. <sup>2</sup>Department of Ophthalmology, Flinders University, Flinders Medical Centre, Bedford Park, South Australia, Australia. <sup>3</sup>South Australian Health and Medical Research Institute, Adelaide, South Australia, Australia.

<sup>4</sup>EMBL Australia Group, Infection & Immunity Theme, South Australian Health and Medical Research Institute, Adelaide, South Australia, Australia.

<sup>5</sup>College of Medicine and Public Health, Flinders University, Bedford Park, South Australia, Australia. <sup>6</sup>Centre for Eye Research Australia, University of Melbourne, Melbourne, Victoria, Australia. <sup>7</sup>Faculty of Medicine and Health Sciences, Macquarie University, Sydney, New South Wales, Australia.

<sup>8</sup>Centre for Vision Research, Westmead Institute for Medical Research, University of Sydney, Sydney, New South Wales, Australia. <sup>9</sup>Discipline of Ophthalmology, Faculty of Medicine & Health Sciences, University of Sydney, Sydney Eye Hospital, Sydney, New South Wales, Australia. <sup>10</sup>South Australian Institute of Ophthalmology, University of Adelaide, Adelaide, South Australia, Australia. <sup>11</sup>Eye Department, Greenlane Clinical Centre, Auckland District Health Board, Auckland, New Zealand. <sup>12</sup>Garvan-Weizmann Centre for Cellular Genomics, Garvan Institute of Medical Research, Sydney, New South Wales, Australia. <sup>13</sup>St Vincent's Clinical School, University of New South Wales, Sydney, New South Wales, Australia. <sup>14</sup>University of Queensland School of Medicine, Brisbane, Queensland, Australia. <sup>15</sup>Institute for Molecular Bioscience, University of Queensland, Brisbane, Queensland, Australia. <sup>16</sup>Menzies Institute for Medical Research, University of Tasmania, Hobart, Tasmania, Australia. <sup>17</sup>Centre for Ophthalmology and Visual Science, University of Western Australia, Crawley, Western Australia, Australia. <sup>18</sup>These authors jointly supervised this work: David A. Mackey, Puya Gharahkhani, Jamie E. Craig, Alex W. Hewitt. \*e-mail: [stuart.macgregor@qimrberghofer.edu.au](mailto:stuart.macgregor@qimrberghofer.edu.au)

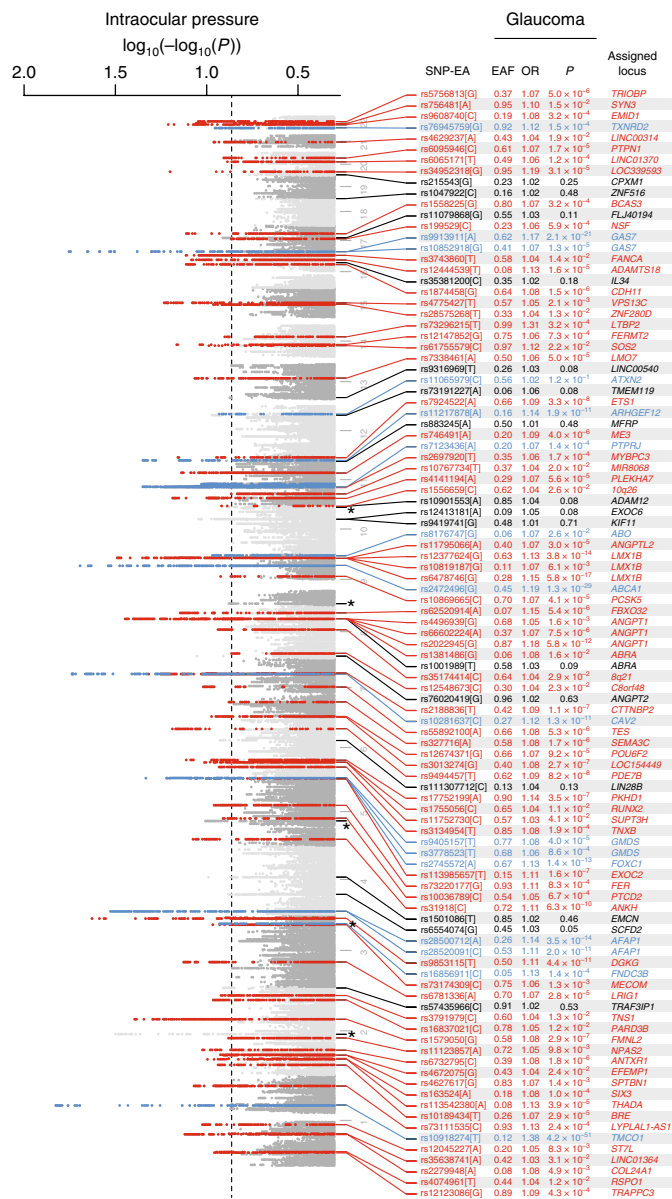


**Fig. 1 | Manhattan plot displaying associations with intraocular pressure in people of Northern European descent.** The dashed line represents the threshold for genome-wide significance ( $P < 5 \times 10^{-8}$ ). Loci highlighted in blue are established regions known to be associated with POAG. The top SNP and its effect allele (SNP-EA) at each genome-wide-significant locus is displayed with the corresponding effect allele frequency (EAF), OR and  $P$  value for association in glaucoma cases (full details in Supplementary Table 1). The results are in black text for SNPs with  $P > 0.05$  with glaucoma, red text for SNPs with  $0.05 < P < 0.05/101$  (not significant after correction for multiple comparisons) and bold red text for SNPs with  $P < 0.05/101$  (significant after correction for multiple comparisons). Asterisk indicates loci that were either reported central corneal thickness loci (ADAMTS6) or more strongly associated with corneal hysteresis and were removed from subsequent analysis (Supplementary Table 2).

been previously associated with IOP, and 16 had been previously associated with either IOP or glaucoma at the genome-wide-significant level<sup>4–12</sup> (marked in blue in Fig. 1). The only previously identified IOP locus that we did not replicate at the genome-wide significant level was ADAMTS8 (peak SNP rs56009602,  $P = 6.2 \times 10^{-6}$ ).

Similarly to other complex traits, additional SNPs beyond the 101 described above are also likely to be associated with IOP but

did not reach genome-wide significance<sup>17</sup>. To estimate the overall contribution of all common variants (i.e., SNP minor allele frequency (MAF)  $> 0.01$ ) to IOP, we applied LD Score regression<sup>18</sup>, which yielded a SNP heritability estimate of 0.16 (s.e.m. = 0.01). We then considered the distribution of association  $P$  values across the genome. Because there was genomic inflation (genomic control  $\lambda = 1.26$ , Supplementary Fig. 3), we computed the LD Score regression intercept to assess whether this genomic inflation was attributable to many variants of small effect (polygenes) or to the effect of issues such as population structure. The LD Score regression intercept was 1.06 (s.e.m. = 0.01), thus indicating that most of the inflation was due to polygenes.

We then performed a GWAS meta-analysis for glaucoma by combining data from UKBB glaucoma cases and controls (selected to be independent of those in our IOP GWAS; 7,947 cases and 119,318 controls) with 3,071 cases from the Australian and New Zealand Registry of Advanced Glaucoma (ANZRAG) and 6,750 historic controls (full description in Methods; Supplementary Fig. 1). Our genome-wide analysis of glaucoma revealed 24 genome-wide-significant loci (Table 1, Supplementary Fig. 4 and Supplementary Fig. 5). With glaucoma, similarly to IOP, there was genomic inflation due to the effect of polygenes (Supplementary Fig. 6), but the intercept of the univariate LD Score regression obtained from the meta-analyzed data was close to 1 (0.95; s.e.m. = 0.01), thus suggesting that our results were not biased by population substructure or cryptic relatedness.

Of the 24 genome-wide-significant loci for glaucoma, two (rs944801 within *CDKN2B-AS1* and rs2093210 within the *SIX6* locus; orange dots in Fig. 2b) are known to be associated with vertical cup-disc ratio (VCDR), an important optic nerve head parameter that is often used to define or diagnose glaucoma<sup>19</sup>. An additional locus (rs61861119 near *MYOF*) was found to have no association with IOP but did have a suggestive level of evidence of association with VCDR<sup>4</sup> ( $P = 1.6 \times 10^{-5}$ ; pink dot in Fig. 2b). The remaining 21 glaucoma loci are likely to influence disease development wholly or partly via IOP, and all showed at least  $P < 0.01$  (15 were genome-wide significant) for IOP (Fig. 2b and Table 1). Of those 21 loci, 7 also showed association with VCDR at  $P < 0.01$  (Table 1).

The relationship between IOP and glaucoma beyond the 24 SNPs that were genome-wide-significantly associated with glaucoma was also examined. At the individual SNP level, of the 101 independent genome-wide-significant IOP SNPs, 53 were significantly associated with glaucoma after Bonferroni correction ( $P < 0.05/101 = 0.000495$ ). The Pearson correlation coefficient between IOP effect size and the glaucoma log(OR) was 0.93 ( $P < 0.001$ ; Fig. 2b). Using bivariate LD Score regression, we estimated the genome-wide genetic correlation between IOP and glaucoma to be 0.71 (s.e.m. = 0.04)<sup>20</sup>.

We also undertook a series of gene-based and pathway-based analyses for IOP and glaucoma. An additional 22 independent genes associated with IOP were identified through FastBAT gene-based tests<sup>21</sup>. Of these 22 genes, 4 were associated with glaucoma after Bonferroni correction for 22 genes ( $P < 0.00227$ ), and an additional 7 achieved  $P < 0.05$  (Supplementary Table 3). In MAGMA pathway analysis<sup>22</sup>, 11 Gene Ontology (GO) annotations were significantly associated with IOP, including extracellular matrix, collagen and vascular development. Among the 11 pathways highlighted by the IOP analysis, 9 showed at least  $P < 0.05$  in pathway analysis in the glaucoma samples, and the strongest GO annotation result was for vascular development ( $P = 0.0015$ ; Supplementary Table 4). Seven pathways were significant in our DEPICT analysis of IOP<sup>23</sup>. The most significant IOP pathways were positive regulation of locomotion, cell motility and cell migration. These pathways were also significant in glaucoma ( $P = 0.0021$ – $0.0025$ ; Supplementary Table 5).

Next, we tested whether the IOP loci could be used to predict POAG in the ANZRAG cohort. Allele scores were derived on the

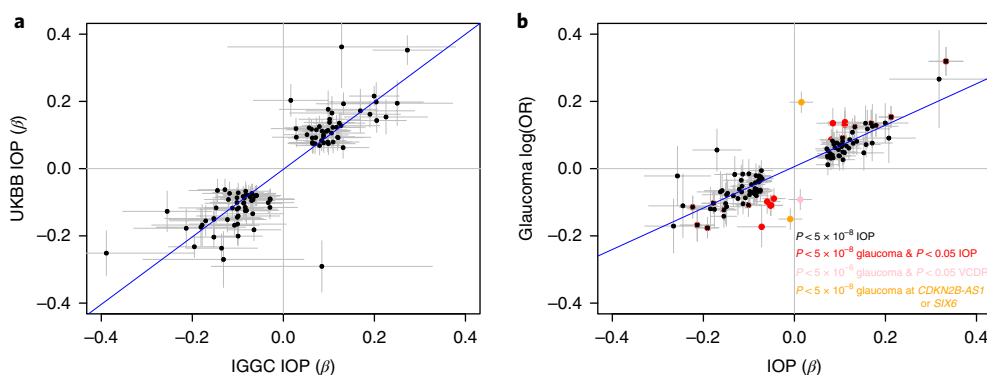


**Fig. 2 | Regression coefficients or effect size for the top associated SNPs at each locus associated with intraocular pressure at the genome-wide-significant level.** Regression coefficients ( $\beta$  in mmHg) are shown, and 95% confidence intervals are displayed in gray. **a**, Comparison of regression coefficients in the UK Biobank (y axis) and the International Glaucoma Genetic Consortium dataset (x axis; Pearson's correlation coefficient = 0.85). The solid line indicates the best fit. **b**, Concordance between regression coefficients for IOP in 133,492 people of Northern European descent (x axis) and the direct effect size ( $\log(\text{OR})$ ) in 11,018 glaucoma cases versus 126,069 controls (y axis; Pearson's correlation coefficient = 0.93). The solid line indicates the line of best fit through the 101 IOP SNPs. The 101 IOP SNPs are shown as black dots. SNPs identified in the GWAS of glaucoma are superimposed in red/pink/orange; those in red show  $P < 0.05$  with IOP; those in pink show  $P < 0.05$  with VCDR but not IOP; the SNPs in orange are at *CDKN2B-AS1* and *SIX6*, which are known to act independently of IOP.

basis of the 101 genome-wide-significant primary IOP SNPs identified in this study (inclusion criteria in Methods) as well as two loci with established associations with optic nerve head morphology (*CDKN2B-AS1* and *SIX6*). These were tested in an independent dataset comprising 1,734 Australians of European ancestry with advanced POAG and 2,938 controls. In comparison to a base model without the allelic scores, the scores were strongly associated with POAG status ( $P < 2 \times 10^{-16}$ , Nagelkerke  $R^2 = 7.7\%$ , area under the curve = 0.65 (95% CI: 0.63–0.66)). Fitting only the IOP and only the VCDR SNPs in the allele score decreased the Nagelkerke  $R^2$  to 5.4% and 2.7%, respectively. Individuals in the top 5%, 10% and 20% of the allele scores were at significantly ( $P < 0.0001$ ) increased risk of POAG relative to the bottom 5%, 10% and 20%, respectively (OR = 7.8, 5.6 and 4.2, respectively).

We sought to characterize the expression profiles of genes at the novel IOP loci that were also associated with glaucoma (Supplementary Fig. 7) across a range of human ocular tissues (corneal epithelium, corneal stroma, corneal endothelium, trabecular meshwork, ciliary body pigmented epithelium, neurosensory retina, optic nerve head and optic nerve). The expression of newly associated genes was more highly enriched ( $P = 6.1 \times 10^{-59}$ , Wilcoxon rank-sum test for novel genes versus all other genes) in the trabecular meshwork compared with other ocular tissues. We then computed the ranks of the novel genes among all genes for each tissue and found that four of the other seven tissues (ciliary body pigmented epithelium, corneal stroma, optic nerve head and optic nerve) were not significantly different, in terms of enrichment, compared with the trabecular meshwork ( $P > 0.05$  for each pairwise comparison, Wilcoxon rank-sum test; the similar tissues are the five leftmost columns in Supplementary Fig. 7). For the other three tissue types (neurosensory retina, corneal epithelium and corneal endothelium, clustered as the three rightmost columns in Supplementary Fig. 7), the degree of enrichment was less than that seen in the trabecular meshwork ( $P < 0.05$  for each pairwise comparison, Wilcoxon rank-sum test). Finally, using FANTOM5 Cap Analysis of Gene Expression data, we found evidence of correlation between enhancers bearing associated SNPs and the promoters of nine genes, including *PTPN1*, *BCLAF1* and *GAS7* in stromal and eye tissues (Supplementary Table 6). This result was noteworthy, given that hypoplasia of the anterior iris stroma is the most common iris defect associated with developmental glaucoma<sup>24</sup> and that these genes may act in a similar, albeit subclinical, manner.

Many of the loci that we identified are associated with other eye conditions. Loss-of-function variants in *LTBP2* have been found to cause primary congenital glaucoma<sup>25</sup>; we now report that common variants at this locus influence IOP in the general population. Similarly, rare loss-of-function variants in *TEK* have been associated with primary congenital glaucoma<sup>26</sup>, and we identified common IOP-influencing variants in genes encoding the two known TEK ligands (*ANGPT1* and *ANGPT2*), as well as a third related protein (*ANGPTL2*).

Anterior segment dysgenesis, iris abnormalities, nanophthalmos and microcornea are known causes of secondary glaucoma<sup>24</sup>. Interestingly, four genes influencing the variation of IOP in the general population have been associated with anterior segment dysgenesis or other abnormalities of the iris, lens or cornea: *FOXC1* with ocular anterior segment dysgenesis; *TRAF3IP1* with iris furrows<sup>27</sup>; *MFRP* with nanophthalmos<sup>28</sup>; and *ADAMTS18* with microcornea, myopic chorioretinal atrophy and telecanthus<sup>29</sup>. Loss-of-function variants in *LMX1B* lead to nail-patella syndrome; common variants at this locus are now definitively associated with both POAG and IOP<sup>30,31</sup>. Interestingly three loci (*PLEKHA7*, *FERMT2* and *GLIS3*) were previously associated with PACG<sup>13,14</sup>, and we have now implicated these regions with IOP; two of those regions (*PLEKHA7* and *FERMT2*) also showed association with POAG (Supplementary Table 1). UKBB participants were not subjected to detailed clinical examination of their ocular anterior segment; hence some associations with IOP or POAG may be at least in part related to undiagnosed narrow drainage angles or subtle variations in ocular development.

Although the Australian glaucoma samples used were confirmed POAG cases<sup>32</sup>, a limitation of the UKBB glaucoma cases was that only a small subset had documented disease subtype. Nevertheless, the proportion of non-POAG glaucoma cases in UKBB would be expected to be small<sup>33</sup>. Applanation-based methods for IOP measurement are influenced by corneal biomechanical properties, such as corneal thickness and hysteresis<sup>34</sup>. A strength of our work is the large sample size for standardized IOP measurement, and corneal compensation data were available for approximately three-quarters of the dataset (corneal compensated IOP data were available for UKBB samples but not for IGGC samples). SNPs more strongly associated with corneal hysteresis than with IOP were excluded, thus allowing us to identify a set of SNPs with greater relevance to glaucoma development rather than spuriously influencing IOP measurement.



**Table 1 | Genome-wide-significant loci identified in meta-analysis of glaucoma (UKBB + ANZTRAG), with their corresponding GWAS statistics from meta-analysis of intraocular pressure (UKBB + IGGC) or vertical cup-disc ratio (IGGC)**

Chromosome	Position	SNP	EA	NEA	OR POAG	95% CI POAG	P POAG	Effect IOP	S.e.m. IOP	P IOP	P VCDR <sup>a</sup>	Nearest gene
1	165736880	rs7518099	T	C	0.73	0.70–0.76	$2.35 \times 10^{-52}$	-0.33	0.02	$3.96 \times 10^{-67}$	0.058	LOC100147773, TMCO1
9	22051670	rs944801	C	G	1.22	1.17–1.27	$8.00 \times 10^{-36}$	0.02	0.01	0.232	$3.85 \times 10^{-32}$	CDKN2B-AS1
9	107695848	rs2472493 <sup>b</sup>	A	G	0.84	0.80–0.87	$4.30 \times 10^{-30}$	-0.19	0.01	$3.62 \times 10^{-50}$	$4.85 \times 10^{-7}$	LOC105376196, ABCA1
14	60957279	rs2093210	T	C	0.86	0.83–0.90	$6.29 \times 10^{-22}$	-0.009	0.01	0.483	$1.22 \times 10^{-9}$	C14orf39, SIX6
17	10031183	rs9913911	A	G	1.16	1.12–1.21	$2.13 \times 10^{-21}$	0.21	0.01	$1.59 \times 10^{-57}$	$5.62 \times 10^{-6}$	GAS7
4	7891545	rs28795989	A	G	1.15	1.11–1.20	$1.90 \times 10^{-20}$	0.15	0.01	$2.94 \times 10^{-32}$	0.019	AFAP1
9	129378026	rs945686	C	G	0.86	0.83–0.90	$2.58 \times 10^{-17}$	-0.14	0.01	$4.25 \times 10^{-22}$	0.016	LMX1B
6	1548369	rs2745572	A	G	1.13	1.08–1.17	$1.35 \times 10^{-13}$	0.13	0.01	$2.66 \times 10^{-22}$	$5.41 \times 10^{-6}$	LOC102723944, GMDS
<b>3</b>	<b>85095766</b>	<b>rs9284802</b>	<b>A</b>	<b>G</b>	<b>0.90</b>	<b>0.86–0.93</b>	<b><math>1.56 \times 10^{-12}</math></b>	<b>-0.05</b>	<b>0.01</b>	<b><math>4.74 \times 10^{-5}</math></b>	<b>0.665</b>	<b>CADM2</b>
11	120248493	rs58073046	A	G	0.85	0.82–0.89	$1.99 \times 10^{-12}$	-0.20	0.02	$1.03 \times 10^{-22}$	0.189	ARHGEF12
<b>7</b>	<b>11679113</b>	<b>rs12699251</b>	<b>A</b>	<b>G</b>	<b>0.90</b>	<b>0.86–0.93</b>	<b><math>4.16 \times 10^{-12}</math></b>	<b>-0.05</b>	<b>0.01</b>	<b><math>9.98 \times 10^{-5}</math></b>	<b>0.100</b>	<b>THSD7A</b>
<b>8</b>	<b>108278616</b>	<b>rs10505100</b>	<b>A</b>	<b>C</b>	<b>0.84</b>	<b>0.81–0.88</b>	<b><math>4.86 \times 10^{-12}</math></b>	<b>-0.21</b>	<b>0.02</b>	<b><math>1.45 \times 10^{-27}</math></b>	<b>0.043</b>	<b>ANGPT1</b>
7	116153025	rs2024211	A	C	0.90	0.86–0.93	$9.48 \times 10^{-12}$	-0.22	0.01	$2.90 \times 10^{-55}$	0.004	CAV1, CAV2
3	186131600	rs9853115	A	T	0.90	0.87–0.94	$4.35 \times 10^{-11}$	-0.18	0.01	$2.84 \times 10^{-43}$	0.026	DGKG, LOC107986164, TBCCD1
<b>5</b>	<b>14851094</b>	<b>rs61394862</b>	<b>T</b>	<b>C</b>	<b>0.90</b>	<b>0.86–0.93</b>	<b><math>4.13 \times 10^{-10}</math></b>	<b>-0.09</b>	<b>0.01</b>	<b><math>8.42 \times 10^{-11}</math></b>	<b>0.781</b>	<b>ANKH</b>
<b>6</b>	<b>170454915</b>	<b>rs2935057</b>	<b>A</b>	<b>G</b>	<b>1.15</b>	<b>1.11–1.20</b>	<b><math>8.02 \times 10^{-10}</math></b>	<b>0.11</b>	<b>0.02</b>	<b><math>1.30 \times 10^{-8}</math></b>	<b>0.250</b>	<b>LOC101929614, LOC105378153</b>
<b>6</b>	<b>637465</b>	<b>rs2073006</b>	<b>T</b>	<b>C</b>	<b>1.14</b>	<b>1.10–1.18</b>	<b><math>1.20 \times 10^{-9}</math></b>	<b>0.11</b>	<b>0.02</b>	<b><math>2.29 \times 10^{-9}</math></b>	<b><math>1.81 \times 10^{-5}</math></b>	<b>EXOC2</b>
10	94942423	rs61861119	A	G	0.91	0.88–0.95	$2.56 \times 10^{-9}$	0.01	0.01	0.313	$1.56 \times 10^{-5}$	MYOF, XRCC6P1
22	19854006	rs8141433	A	G	1.15	1.11–1.20	$3.04 \times 10^{-9}$	0.08	0.02	$2.85 \times 10^{-6}$	0.235	TXNRD2
<b>10</b>	<b>60338753</b>	<b>rs4141671</b>	<b>T</b>	<b>C</b>	<b>0.91</b>	<b>0.88–0.95</b>	<b><math>8.67 \times 10^{-9}</math></b>	<b>-0.05</b>	<b>0.01</b>	<b>0.0004</b>	<b>0.0001</b>	<b>BICC1</b>
<b>3</b>	<b>169252883</b>	<b>rs73174345</b>	<b>T</b>	<b>G</b>	<b>0.84</b>	<b>0.80–0.89</b>	<b><math>1.53 \times 10^{-8}</math></b>	<b>-0.07</b>	<b>0.03</b>	<b>0.008</b>	<b>0.732</b>	<b>MECOM</b>
<b>7</b>	<b>117603820</b>	<b>rs1013278</b>	<b>C</b>	<b>G</b>	<b>1.09</b>	<b>1.05–1.14</b>	<b><math>2.99 \times 10^{-8}</math></b>	<b>0.08</b>	<b>0.01</b>	<b><math>3.32 \times 10^{-10}</math></b>	<b>0.003</b>	<b>CTTNBP2, CFTR</b>
<b>11</b>	<b>128380742</b>	<b>rs7924522</b>	<b>A</b>	<b>C</b>	<b>1.09</b>	<b>1.05–1.14</b>	<b><math>3.33 \times 10^{-8}</math></b>	<b>0.11</b>	<b>0.01</b>	<b><math>3.99 \times 10^{-15}</math></b>	<b>0.090</b>	<b>ETS1</b>
<b>3</b>	<b>150059342</b>	<b>rs11710139</b>	<b>A</b>	<b>G</b>	<b>0.90</b>	<b>0.87–0.94</b>	<b><math>5.00 \times 10^{-8}</math></b>	<b>-0.06</b>	<b>0.01</b>	<b><math>3.89 \times 10^{-5}</math></b>	<b>0.463</b>	<b>LOC107986141, LOC107986142</b>

The results are presented from the smallest to the largest *P* value for glaucoma. Bold indicates previously unreported risk loci for primary open-angle glaucoma. EA, effect allele; NEA, non-effect allele.

<sup>a</sup>*P* value obtained from the VCDR GWAS in IGGC. <sup>b</sup>This SNP was not present in the IOP data passing quality control; hence, the corresponding statistics for IOP is reported for rs2472496 (effect allele A, non-effect allele G), a SNP in high linkage disequilibrium ( $r^2 = 0.967$ ) with rs2472493.

In conclusion, we leveraged large sample sets from the UKBB and the IGGC to dramatically expand the number of genomic regions associated with IOP. We identified 101 statistically independent SNPs for IOP and found that 53 of them were associated with glaucoma. This work highlights the high genetic correlation between IOP and glaucoma. A number of previously implicated (extracellular matrix and collagen) and novel (vascular development and cell migration) pathways were associated with both IOP and glaucoma. Finally, an allele score based on the IOP loci and loci influencing optic nerve head morphology was able to enhance risk stratification.

**URLs.** BOLT-LMM, <https://data.broadinstitute.org/alkesgroup/BOLT-LMM/>; DEPICT, <https://data.broadinstitute.org/mpg/depiect/index.html>; Drug Gene Interaction Database, <http://dgidb.genome.wustl.edu/>; EdgeR Bioconductor package, <https://bioconductor.org/packages/release/bioc/html/edgeR.html>; FANTOM5 data, <http://enhancer.binf.ku.dk/>; GCTA software, <http://cnsngomics.com/software/gcta/>; Haplotype Reference Consortium, <http://www.haplotype-reference-consortium.org/>; International Glaucoma Genetic Consortium dataset, <https://cloudstor.aarnet.edu.au/plus/s/O9RU6zrQbpyHCSe/>; HTSeq-count v0.6.0 software, <https://pypi.python.org/pypi/HTSeq/>; LOCUSZOOM, <http://locuszoom.sph.umich.edu/>; LD-hub database, <http://ldsc.broadinstitute.org/>; MAGMA, <https://ctg.cncr.nl/software/magma/>; METAL software, <http://csg.sph.umich.edu/abecasis/Metal/>; PLINK software, <http://www.cog-genomics.org/plink2/>; TopHat v2.1.1 software, <https://ccb.jhu.edu/software/tophat/index.shtml>; UK Biobank, <http://www.ukbiobank.ac.uk/>.

**Methods**  
Methods, including statements of data availability and any associated accession codes and references, are available at <https://doi.org/10.1038/s41588-018-0176-y>.

Received: 21 August 2017; Accepted: 13 June 2018;  
Published online: 27 July 2018

## References

- Weinreb, R. N. et al. Primary open-angle glaucoma. *Nat. Rev. Dis. Prim.* **2**, 16067 (2016).
- Sanfilippo, P. G., Hewitt, A. W., Hammond, C. J. & Mackey, D. A. The heritability of ocular traits. *Surv. Ophthalmol.* **55**, 561–583 (2010).
- Bycroft, C. et al. Genome-wide genetic data on ~500,000 UK Biobank participants. Preprint at <https://www.biorxiv.org/content/early/2017/07/20/166298/> (2017).
- Springelkamp, H. et al. New insights into the genetics of primary open-angle glaucoma based on meta-analyses of intraocular pressure and optic disc characteristics. *Hum. Mol. Genet.* **26**, 438–453 (2017).
- van Koolwijk, L. M. E. et al. Common genetic determinants of intraocular pressure and primary open-angle glaucoma. *PLoS Genet.* **8**, e1002611 (2012).
- Springelkamp, H. et al. ARHGEF12 influences the risk of glaucoma by increasing intraocular pressure. *Hum. Mol. Genet.* **24**, 2689–2699 (2015).
- Bailey, J. N. C. et al. Genome-wide association analysis identifies TXNRD2, ATXN2 and FOXC1 as susceptibility loci for primary open-angle glaucoma. *Nat. Genet.* **48**, 189–194 (2016).
- Gharahkhani, P. et al. Common variants near *ABCA1*, *AFAP1* and *GMD5* confer risk of primary open-angle glaucoma. *Nat. Genet.* **46**, 1120–1125 (2014).
- Hysi, P. G. et al. Genome-wide analysis of multi-ancestry cohorts identifies new loci influencing intraocular pressure and susceptibility to glaucoma. *Nat. Genet.* **46**, 1126–1130 (2014).
- Chen, Y. et al. Common variants near *ABCA1* and in *PMM2* are associated with primary open-angle glaucoma. *Nat. Genet.* **46**, 1115–1119 (2014).
- Burdon, K. P. et al. Genome-wide association study identifies susceptibility loci for open angle glaucoma at *TMC01* and *CDKN2B-AS1*. *Nat. Genet.* **43**, 574–578 (2011).
- Thorleifsson, G. et al. Common variants near *CAV1* and *CAV2* are associated with primary open-angle glaucoma. *Nat. Genet.* **42**, 906–909 (2010).
- Vithana, E. N. et al. Genome-wide association analyses identify three new susceptibility loci for primary angle closure glaucoma. *Nat. Genet.* **44**, 1142–1146 (2012).
- Khor, C. C. et al. Genome-wide association study identifies five new susceptibility loci for primary angle closure glaucoma. *Nat. Genet.* **48**, 556–562 (2016).
- Yang, J. et al. Conditional and joint multiple-SNP analysis of GWAS summary statistics identifies additional variants influencing complex traits. *Nat. Genet.* **44**, 369–375 (2012).
- Lu, Y. et al. Genome-wide association analyses identify multiple loci associated with central corneal thickness and keratoconus. *Nat. Genet.* **45**, 155–163 (2013).
- Yang, J. et al. Common SNPs explain a large proportion of the heritability for human height. *Nat. Genet.* **42**, 565–569 (2010).
- Bulik-Sullivan, B. K. et al. LD Score regression distinguishes confounding from polygenicity in genome-wide association studies. *Nat. Genet.* **47**, 291–295 (2015).
- Ramdas, W. D. et al. A genome-wide association study of optic disc parameters. *PLoS Genet.* **6**, e1000978 (2010).
- Bulik-Sullivan, B. et al. An atlas of genetic correlations across human diseases and traits. *Nat. Genet.* **47**, 1236–1241 (2015).
- Bakshi, A. et al. Fast set-based association analysis using summary data from GWAS identifies novel gene loci for human complex traits. *Sci. Rep.* **6**, 32894 (2016).
- de Leeuw, C. A., Mooij, J. M., Heskes, T. & Posthuma, D. MAGMA: generalized gene-set analysis of GWAS data. *PLOS Comput. Biol.* **11**, e1004219 (2015).
- Pers, T. H. et al. Biological interpretation of genome-wide association studies using predicted gene functions. *Nat. Commun.* **6**, 5890 (2015).
- Reis, L. M. & Semina, E. V. Genetics of anterior segment dysgenesis disorders. *Curr. Opin. Ophthalmol.* **22**, 314–324 (2011).
- Ali, M. et al. Null mutations in *LTBP2* cause primary congenital glaucoma. *Am. J. Hum. Genet.* **84**, 664–671 (2009).
- Souma, T. et al. Angiopoietin receptor TEK mutations underlie primary congenital glaucoma with variable expressivity. *J. Clin. Invest.* **126**, 2575–2587 (2016).
- Larsson, M. et al. GWAS findings for human iris patterns: associations with variants in genes that influence normal neuronal pattern development. *Am. J. Hum. Genet.* **89**, 334–343 (2011).
- Sundin, O. H. et al. Extreme hyperopia is the result of null mutations in *MFRP*, which encodes a Frizzled-related protein. *Proc. Natl. Acad. Sci. USA* **102**, 9553–9558 (2005).
- Khan, A. O. Microcornea with myopic chorioretinal atrophy, telecanthus and posteriorly-rotated ears: a distinct clinical syndrome. *Ophthalmic Genet.* **33**, 196–199 (2012).
- Vollrath, D. et al. Loss-of-function mutations in the LIM-homeodomain gene, *LMX1B*, in nail-patella syndrome. *Hum. Mol. Genet.* **7**, 1091–1098 (1998).
- Sweeney, E., Fryer, A., Mountford, R., Green, A. & McIntosh, I. Nail patella syndrome: a review of the phenotype aided by developmental biology. *J. Med. Genet.* **40**, 153–162 (2003).
- Souzeau, E. et al. Australian and New Zealand Registry of Advanced Glaucoma: methodology and recruitment. *Clin. Exp. Ophthalmol.* **40**, 569–575 (2012).
- Quigley, H. A. & Broman, A. T. The number of people with glaucoma worldwide in 2010 and 2020. *Br. J. Ophthalmol.* **90**, 262–267 (2006).
- Ehlers, N., Bramsen, T. & Sperling, S. Applanation tonometry and central corneal thickness. *Acta Ophthalmol. (Copenh.)* **53**, 34–43 (1975).

## Acknowledgements

This work was conducted by using the UK Biobank Resource (application number 25331) and publicly available data from the International Glaucoma Genetics Consortium. This work was supported by grants from the National Health and Medical Research Council (NHMRC) of Australia (1107098 (J.E.C.), 1116360 (D.A.M.), 1116495 (J.E.C.) and 1023911 (D.A.M.)), the Ophthalmic Research Institute of Australia and the BrightFocus Foundation. S.M. is supported by an Australian Research Council Future Fellowship. K.P.B., J.E.C. and A.W.H. are supported by NHMRC Fellowships. D.J.L. is supported by an EMBL Australia group leader award. We thank S. Wood and J. Pearson from QIMR Berghofer for IT support.

## Author contributions

S.M., A.W.H., J.E.C., P.G. and D.A.M. designed the study and obtained funding. S.M., J.S.O., J.A., X.H., T.Z., M.H.L., S.S., J.E.P., D.L. and J.B. analyzed the data. S.M., T.Z., O.S., E.S., S.S., B.S., R.A.M., J.L., J.B.R., S.L.G., P.R.H., A.J.R.W., R.J.C., S.B., J.R.G., I.G., D.C.W., G.R.S., N.G.M., G.W.M., K.P.B., D.A.M., J.E.C. and A.W.H. contributed to data collection and contributed to genotyping. S.M., J.S.O., D.A.M., P.G. and A.W.H. wrote the first draft of the paper. All authors contributed to the final version of the paper.

## Competing interests

The authors declare no competing interests.

## Additional information

**Supplementary information** is available for this paper at <https://doi.org/10.1038/s41588-018-0176-y>.

**Reprints and permissions information** is available at [www.nature.com/reprints](http://www.nature.com/reprints).

**Correspondence and requests for materials** should be addressed to S.M.

**Publisher's note:** Springer Nature remains neutral with regard to jurisdictional claims in published maps and institutional affiliations.

## Methods

**Analysis of UK Biobank data.** A complete description of the UKBB genotype curation can be found in the report by Bycroft and colleagues<sup>3</sup>. All participants provided informed written consent, the study was approved by the National Research Ethics Service Committee North West–Haydock, and all study procedures were performed in accordance with the World Medical Association Declaration of Helsinki ethical principles for medical research. In brief, approximately 488,000 participants were genotyped on custom-designed Affymetrix UK BiLEVE Axiom or UK Biobank Axiom arrays (Affymetrix), which produced a combined total of 805,426 markers in the released data. After standard quality control (QC), the dataset was phased, and ~96 million genotypes were imputed with Haplotype Reference Consortium (HRC; see URLs) and UK10K haplotype resources<sup>3,35,36</sup>. Owing to the UKBB's reported QC issues with non-HRC SNPs, we retained only the ~40 million HRC SNPs for analysis.

Among the 487,409 individuals who passed initial genotyping QC, 409,694 participants had white British ancestry, according to self-reported ethnicity and genetic principal components. To maximize our effective sample size, we also included UKBB participants if their self-reported ancestry was not white British (including a substantial number of individuals reporting their ancestry as 'Irish' or 'any other white background'), but their first two genetic principal components fell within the region of those classified as white British in the  $n=409,694$  set in Bycroft *et al.*<sup>3</sup> (Supplementary Fig. 8). With these criteria, we identified 438,870 individuals for this study who were genetically similar to those of white-British ancestry.

Individuals were selected for analysis to ensure the independence of the IOP and glaucoma arms of the study. Selection was based on the following criteria (Supplementary Fig. 1): (i) glaucoma cases were selected; (ii) individuals participating in the ocular examination (approximately one-quarter of the UKBB cohort) were selected (with glaucoma cases and their relatives ( $\hat{\pi} > 0.2$ )) omitted; and (iii) individuals who self-reported having no eye disease were selected (controls were screened to be unrelated ( $\hat{\pi} > 0.2$ )) for use as controls with the glaucoma cases. Among the 438,870 individuals with suitable genetic data, we extracted 7,947 individuals with glaucoma; cases were those who (i) had an ICD-10 diagnosis of 'primary open angle glaucoma', 'other glaucoma' or 'glaucoma, unspecified'; (ii) responded 'glaucoma' to the question 'Has a doctor told you that you have any of the following problems with your eyes?'; or (iii) responded 'glaucoma' to the question 'In the touch screen you selected that you have been told by a doctor that you have other serious illnesses or disabilities, could you now tell me what they are? (non-cancer illness)'. Although this glaucoma definition is broad, ~80% of 'glaucoma' cases among white British individuals are likely to meet the diagnostic criteria for POAG<sup>33</sup>. The number of individuals with ICD-10 POAG was more than five times fewer, thus limiting the power of the study. A subset (127,468) of UKBB participants took part in the ocular examination, which included IOP measurements with the Ocular Response Analyzer noncontact tonometer<sup>37</sup>. Our primary IOP analysis was based on corneal-compensated IOP (IOPcc) measurements, because these are expected to be less affected by corneal factors than Goldmann-correlated IOP measures. The mean IOPcc for each participant was calculated, and measurements  $< 5$  or  $> 60$  mmHg were set to 'missing'. Mean corneal hysteresis and mean non-corneal-compensated (Goldmann-correlated) IOP were also derived and tested at loci of interest from the IOPcc analysis. 103,914 individuals with ocular examinations had both phenotype and genotype data available. Finally, controls for the glaucoma cases were selected on the basis of a reply of 'none' to the question 'Has a doctor told you that you have any of the following problems with your eyes?' and no ocular examination.

**Genotyping and analysis of the Australian & New Zealand Registry of Advanced Glaucoma (ANZRAG) Cohort.** The clinical recruitment and characterization of the ANZRAG cohort has been described previously<sup>32</sup>. In this analysis, a total of 3,071 POAG cases and 6,750 historic controls of European descent were used. Case and control samples were genotyped on Illumina Omni1M, OmniExpress or HumanCoreExome arrays (Illumina)<sup>8,11</sup>. This dataset involved three phases of POAG data collection, and hence, QC, imputation and association analysis were conducted separately for each phase before the results were combined in a meta-analysis. The first phase was previously published and comprised 1,155 advanced POAG cases and 1,992 historic controls genotyped on Illumina Omni1M or OmniExpress arrays<sup>11</sup>. In that phase, the historic controls were obtained from 225 esophageal cancer cases, 317 Barrett's esophagus cases and their 552 controls, as well as 303 inflammatory bowel disease cases and their corresponding cohort of 595 controls. The second phase included a further 579 advanced POAG cases genotyped on the Illumina HumanCoreExome array and 946 controls selected from parents of twins previously genotyped on the same array<sup>8</sup>. The third phase comprised 1,337 POAG cases genotyped on the Illumina HumanCoreExome array and 3,812 controls selected from a study of endometriosis previously genotyped on the same array<sup>38</sup>. There is strong female bias in the control set in phase three, but not in phases one and two (our allele-score prediction described below used only phases one and two). Human research ethics approval was obtained from the relevant committees of the Southern Adelaide Clinical Human Research Ethics Committee/Flinders University, the University of Tasmania, QIMR Berghofer Institute of Medical Research and the Royal Victorian Eye and Ear Hospital.

Written informed consent was obtained from all participants in accordance with the Declaration of Helsinki.

As described previously, QC was performed with PLINK (see URLs)<sup>39</sup>. Individuals with more than 3% missing genotypes and SNPs with a call rate  $< 97\%$ ,  $MAF < 0.01$  and Hardy–Weinberg-equilibrium  $P < 0.0001$  in controls or  $P < 5 \times 10^{-10}$  in cases were removed from the analysis. Identity by descent was determined on the basis of autosomal markers in PLINK<sup>39</sup>, and only one of each pair of individuals with relatedness ( $\hat{\pi}$ )  $> 0.2$  was used in the analysis. PLINK was used to compute principal components for all participants and reference samples of known northern European ancestry (1000G British, CEU and Finland participants). Participants with PC1 or PC2 values more than six s.d. from the mean of the known Northern European ancestry group were excluded. All statistical tests throughout the manuscript were two sided.

Phasing of the genotyped SNPs was conducted with ShapeIT<sup>40</sup>, and imputation was performed with Minimac3 through the Michigan Imputation Server<sup>41</sup>, with the HRC as the reference panel<sup>35</sup>. SNPs with imputation quality ( $\hat{r}^2$ )  $> 0.3$  and  $MAF > 0.01$  were used for analysis.

**Association testing.** *IOP IGGC.* We obtained publicly available GWAS summary statistics from an IGGC study on IOP<sup>4</sup>. 29,578 individuals had 1000G imputed GWAS data available, with IOP corrected for age and sex<sup>4</sup>. Most IGGC sites used Goldmann-corrected IOP; these IOP measures do not account for corneal differences between individuals, and in large samples an 'IOP' analysis may identify loci that are primarily driven by corneal parameters<sup>4</sup>.

*IOP UKBB.* Association analysis was performed with a linear mixed-model framework to account for cryptic relatedness and population stratification in the UKBB samples with BOLT-LMM version 2.3 (see URLs)<sup>42</sup>. We used a sparse set of 360,087 genotyped SNPs across the autosomes to estimate the Bayesian Gaussian mixture before characterizing the random-effects genetic component. The infinitesimal model in BOLT-LMM was used to generate GWAS  $P$  values. The IGGC and UKBB IOP results were combined with meta-analysis implemented in METAL<sup>43</sup> (25 March 2011 release; see URLs).

To identify statistically independent genome-wide-significant SNPs, an initial list of SNPs with meta-analysis  $P$  values  $< 5 \times 10^{-8}$  was pruned into discrete regions by linkage disequilibrium (LD) clumping in PLINK v1.9 ( $r^2$  threshold for clumping, 0.1; physical distance threshold for clumping, 2 Mb). This initial list of SNPs was then further explored for additional independent signals by conditioning the meta-analysis summary data with GCTA version 1.26 (see URLs). To calculate LD, a reference panel was constructed from 5,000 individuals randomly selected from the UKBB individuals of white British ancestry. Imputed SNPs with  $r^2 > 0.3$  and  $MAF > 0.001$  were converted to best-guess genotypes, then cleaned for 3% missingness and Hardy–Weinberg equilibrium  $< 1 \times 10^{-6}$ . Initially, a given peak SNP was used to condition all SNPs within 2 Mb (--cojo-cond option). When there were multiple SNPs within 2 Mb of each other, they were analyzed together with boundaries at least  $\pm 2$  Mb from the furthest SNP. Subsequently, an SNP was deemed independent if its initial single SNP  $P$  value was  $< 5 \times 10^{-8}$  and remained  $< 5 \times 10^{-8}$  after conditioning. Newly identified SNPs were iteratively added to the regional conditioning until no more SNPs had a  $P$  value  $< 5 \times 10^{-8}$ . As a final check, the joint effect (--cojo-joint) of all putatively genome-wide-significant SNPs was estimated, and any SNPs that had joint  $P$  values  $> 5 \times 10^{-8}$  were discarded.

**UK Biobank glaucoma case–control analysis.** We assessed associations between SNPs and glaucoma status adjusted for sex and the first six principal components, under an additive genetic model with the dosage scores obtained from imputation. Association analysis was performed with PLINK version 2.0 (ref. <sup>39</sup>). Identity by descent was determined on the basis of autosomal markers in PLINK version 1.90b, and only one of each pair of individuals with  $\hat{\pi} > 0.2$  was used in the analysis. Figure 1 was produced with Adobe Illustrator to juxtapose a Manhattan plot in R with a table produced in R.

We used the mean  $\chi^2$  and the univariate LD Score regression approach to investigate the presence of model or structural bias in the glaucoma GWAS data<sup>18</sup>. An LD Score intercept close to 1 in a univariate analysis indicates that there is no model misspecification and that other sources of bias, such as population stratification and cryptic relatedness, are not adversely affecting the results.

**Exclusion of loci on the basis of association with corneal parameters.** All loci that were genome-wide-significantly associated with IOP were tested for association with corneal hysteresis (hyst, a measure of viscous damping in the cornea that may affect the measurement of IOP). SNPs with a larger effect on hyst than on IOP are unlikely to be truly associated with IOP, and hence we filtered SNPs with  $P_{\text{hyst}} < P_{\text{IOP}}$  (SNPs with effects on various aspects of eye morphology of large effect, such as *TMCO1*, influenced both IOP and hyst, and so we did not filter simply on  $P_{\text{hyst}}$ ). Similarly, putative IOP loci were examined for previous association with central corneal thickness<sup>16</sup>.

**LD Score regression.** We applied univariate LD Score regression (see URLs)<sup>18</sup> to estimate the SNP heritability of IOP and used bivariate LD Score regression<sup>20</sup> to estimate the genetic correlation between IOP and glaucoma.

**Gene-based tests.** Gene-based tests were conducted with the fast and flexible set-based association test (FastBAT), a gene-based approach that calculates the association  $P$  values for a set of SNPs (within  $\pm 50$  kb of a gene in this study) with GWAS summary data while accounting for LD between SNPs<sup>21</sup>. Only loci distinct from those found in the per-SNP tests ( $> 1$  Mb away) were tested. FastBAT was applied to the IOP meta-analysis results, with a significance threshold of  $2 \times 10^{-6}$  (0.05/24,654 genes tested). Genes exceeding this threshold were then tested for association with glaucoma (ANZTRAG + UKBB) with FastBAT.

**Pathway-based tests.** Pathway-based tests were conducted on the IOP meta-analysis results with MAGMA and DEPICT (see URLs)<sup>23,44</sup>. We opted to use both approaches because they use different pathway databases as well as a different method for annotating SNPs to genes. In MAGMA,  $Z$  scores from a gene-based step were combined on the basis of 5,917 prespecified GO gene sets. DEPICT is an integrative tool that, for each gene, uses the likelihood of membership in each gene set, according to the co-regulation of gene expression data, and tests whether any of the 14,462 preconstituted gene sets are significantly enriched in genes in the trait-associated loci. SNPs exceeding  $P < 5 \times 10^{-8}$  were used to define trait-associated loci in a pathway analysis in DEPICT. Pathways exceeding  $P < 0.05/5,917$  (MAGMA) or  $P < 0.05/14,463$  (DEPICT) were then tested with the same approach in glaucoma (ANZTRAG + UKBB).

**Allele scores.** We used the allele-score approach to investigate whether the genome-wide-significant IOP loci identified in this study, as well as the two previously known VCDR loci with established association with POAG (rs2157719 within the *CDKN2B-AS1* locus and rs8015152 within the *SIX6* locus), were able to significantly predict the risk of glaucoma. We used only statistically independent SNPs to create the profile scores and excluded the known published central corneal thickness loci as well as corneal hysteresis SNPs, whose  $P$  values in this study were lower than the IOP  $P$  values. This procedure was performed to rule out those SNPs that might not truly affect IOP but have been detected as IOP loci because of their effects on corneal hysteresis. The SNPs passing the above criteria were used to score individuals in a target cohort, a subset of the ANZTRAG data with advanced POAG (1,734 cases and 2,938 controls). Our ANZTRAG dataset was nonoverlapping with the cohort used to identify the IOP SNPs (and their estimated effect sizes). The score for each individual in ANZTRAG was calculated by summing the number of risk alleles weighted by their effect sizes obtained from the IOP and VCDR analyses. Because IOP and VCDR are measured on different scales, we benchmarked their relative weights (in terms of their effect on glaucoma) with the well-established large effect associations with IOP (*TMC01* rs10918274, estimated to increase IOP by 0.33 units and in a POAG meta-analysis, to increase risk 1.39 fold) and with VCDR (*CDKN2B-AS1* rs2157719, estimated to increase VCDR by 0.13 and POAG 1.44 fold)<sup>4</sup>. According to these benchmarks, each unit increase in IOP leads to a  $0.998 \log(\text{OR})$  increase ( $\log(1.39)/0.33$ ) in POAG risk. Similarly, each unit increase in VCDR leads to a  $28.049 \log(\text{OR})$  increase ( $\log(1.44)/0.13$ ) in POAG risk. Hence, before combining the IOP and VCDR allele scores for analysis, we multiplied the VCDR risk score by  $28.049/0.998$  to place it on an equivalent scale to IOP.

To estimate the contribution of the profile scores to the POAG status in the ANZTRAG target cohort, we first performed a logistic regression with sex and the first four principal components used as covariates (base model). We then added the profile scores into the logistic model and computed the increase in Nagelkerke's pseudo  $R^2$  from the logistic regression over and above the base model (Nagelkerke's pseudo  $R^2$  is a measure of the goodness of fit in the prediction model and is analogous to phenotypic variance explained in a linear regression). We also compared the POAG risk for the top versus bottom 5%, 10% (decile) and 20% of the profile-score distribution.

**Drug pathway.** The Drug Gene Interaction Database (DGIdb 3.0 release; see URLs) was used to identify compounds that act on genes at each locus and could be repurposed in the treatment of glaucoma<sup>45</sup>.

**Gene target prediction.** FANTOM5 data representing enhancer-promoter cap analysis of gene expression (CAGE) expression correlation from all cell types were downloaded and processed (see URLs)<sup>44</sup>. Enhancers active in eye and stromal

tissues were tested for overlap with SNPs correlated with lead SNPs ( $r^2 > 0.8$  in 1000Genomes EUR populations). Genes for which CAGE promoter expression signals were correlated with enhancers were selected as potential target genes.

**Ocular expression analysis.** The gene expression profiles of all genes within IOP-associated loci were examined in relevant ocular tissues. Data were available from a total of 16 donor eyes from 16 individuals. RNA was extracted from 48 samples of distinct ocular tissue (corneal epithelium, corneal stroma, corneal endothelium, trabecular meshwork, ciliary body pigmented epithelium, neurosensory retina, optic nerve head and optic nerve) and sequenced with the Illumina NextSeq 500 platform (FC-404-2005) with a Bioo Scientific NEXTflex rapid directional mRNA-seq kit (5138-10). We obtained an average of 56 million 75-bp paired-end reads per sample. After QC and trimming, these were mapped to the reference human genome (hg19) with TopHat v2.1.1 and HTSeq-count v0.6.0 (see URLs)<sup>46,47</sup>. Normalized counts-per-million data were calculated with the trimmed mean of  $M$  values (TMM) normalization method with edgeR v3.10.2 (see URLs)<sup>48</sup>. Transcripts from a total of 21,962 RefSeq protein-coding genes were captured and mapped. After QC filtering, 94.5% of the reads mapped to the human genome. The mean TMM value across all available samples for each gene in each tissue was calculated. To test whether there was enrichment for genes at the novel loci associated with glaucoma in each tissue, we used a Wilcoxon rank-sum test for novel genes versus all other genes. We then computed the ranks of the novel genes among all genes for each tissue and compared each tissue in turn to the tissue showing most enrichment (Wilcoxon rank-sum test).

**Reporting Summary.** Further information on experimental design is available in the Nature Research Reporting Summary linked to this article.

**Data availability.** The data that support the findings of this study are available from the corresponding author upon reasonable request. International Glaucoma Genetic Consortium results are available from <https://cloudstor.aarnet.edu.au/plus/s/O9RU6zrQbpyHCSe/>. UK Biobank data are available through the UK Biobank Access Management System (see URLs).

## References

- McCarthy, S. et al. A reference panel of 64,976 haplotypes for genotype imputation. *Nat. Genet.* **48**, 1279–1283 (2016).
- UK10K Consortium. The UK10K project identifies rare variants in health and disease. *Nature* **526**, 82–90 (2015).
- Chan, M. P. Y. et al. Associations with intraocular pressure in a large cohort: results from the UK Biobank. *Ophthalmology* **123**, 771–782 (2016).
- Kneehole, D. R. et al. Genome-wide association meta-analysis identifies new endometriosis risk loci. *Nat. Genet.* **44**, 1355–1359 (2012).
- Purcell, S. et al. PLINK: a tool set for whole-genome association and population-based linkage analyses. *Am. J. Hum. Genet.* **81**, 559–575 (2007).
- Delaneau, O., Marchini, J. & Zagury, J.-F. A linear complexity phasing method for thousands of genomes. *Nat. Methods* **9**, 179–181 (2011).
- Das, S. et al. Next-generation genotype imputation service and methods. *Nat. Genet.* **48**, 1284–1287 (2016).
- Loh, P.-R. et al. Efficient Bayesian mixed-model analysis increases association power in large cohorts. *Nat. Genet.* **47**, 284–290 (2015).
- Willer, C. J. et al. Newly identified loci that influence lipid concentrations and risk of coronary artery disease. *Nat. Genet.* **40**, 161–169 (2008).
- Andersson, R. et al. An atlas of active enhancers across human cell types and tissues. *Nature* **507**, 455–461 (2014).
- Griffith, M. et al. DGIdb: mining the druggable genome. *Nat. Methods* **10**, 1209–1210 (2013).
- Kim, D. et al. TopHat2: accurate alignment of transcriptomes in the presence of insertions, deletions and gene fusions. *Genome Biol.* **14**, R36 (2013).
- Anders, S., Pyl, P. T. & Huber, W. HTSeq: a Python framework to work with high-throughput sequencing data. *Bioinformatics* **31**, 166–169 (2015).
- McCarthy, D. J., Chen, Y. & Smyth, G. K. Differential expression analysis of multifactor RNA-Seq experiments with respect to biological variation. *Nucleic Acids Res.* **40**, 4288–4297 (2012).



## Reporting Summary

Nature Research wishes to improve the reproducibility of the work that we publish. This form provides structure for consistency and transparency in reporting. For further information on Nature Research policies, see [Authors & Referees](#) and the [Editorial Policy Checklist](#).

### Statistical parameters

When statistical analyses are reported, confirm that the following items are present in the relevant location (e.g. figure legend, table legend, main text, or Methods section).

n/a Confirmed

- ☐ ☒ The exact sample size ( $n$ ) for each experimental group/condition, given as a discrete number and unit of measurement
- ☐ ☒ An indication of whether measurements were taken from distinct samples or whether the same sample was measured repeatedly
- ☐ ☒ The statistical test(s) used AND whether they are one- or two-sided  
*Only common tests should be described solely by name; describe more complex techniques in the Methods section.*
- ☐ ☒ A description of all covariates tested
- ☐ ☒ A description of any assumptions or corrections, such as tests of normality and adjustment for multiple comparisons
- ☐ ☒ A full description of the statistics including central tendency (e.g. means) or other basic estimates (e.g. regression coefficient) AND variation (e.g. standard deviation) or associated estimates of uncertainty (e.g. confidence intervals)
- ☐ ☒ For null hypothesis testing, the test statistic (e.g.  $F$ ,  $t$ ,  $r$ ) with confidence intervals, effect sizes, degrees of freedom and  $P$  value noted  
*Give  $P$  values as exact values whenever suitable.*
- ☒ ☐ For Bayesian analysis, information on the choice of priors and Markov chain Monte Carlo settings
- ☒ ☐ For hierarchical and complex designs, identification of the appropriate level for tests and full reporting of outcomes
- ☐ ☒ Estimates of effect sizes (e.g. Cohen's  $d$ , Pearson's  $r$ ), indicating how they were calculated
- ☒ ☐ Clearly defined error bars  
*State explicitly what error bars represent (e.g. SD, SE, CI)*

Our web collection on [statistics for biologists](#) may be useful.

### Software and code

Policy information about [availability of computer code](#)

Data collection Described in detail in the methods section.

Data analysis Described in detail in the methods section.

For manuscripts utilizing custom algorithms or software that are central to the research but not yet described in published literature, software must be made available to editors/reviewers upon request. We strongly encourage code deposition in a community repository (e.g. GitHub). See the Nature Research [guidelines for submitting code & software](#) for further information.

### Data

Policy information about [availability of data](#)

All manuscripts must include a [data availability statement](#). This statement should provide the following information, where applicable:

- Accession codes, unique identifiers, or web links for publicly available datasets
- A list of figures that have associated raw data
- A description of any restrictions on data availability

The International Glaucoma Genetics Consortium summary statistics are publicly available (reference in previous publication). The UK Biobank data is available to investigators upon application via <http://www.ukbiobank.ac.uk/>



## Field-specific reporting

Please select the best fit for your research. If you are not sure, read the appropriate sections before making your selection.

☒ Life sciences ☐ Behavioural & social sciences ☐ Ecological, evolutionary & environmental sciences

For a reference copy of the document with all sections, see [nature.com/authors/policies/ReportingSummary-flat.pdf](https://www.nature.com/authors/policies/ReportingSummary-flat.pdf)

## Life sciences study design

All studies must disclose on these points even when the disclosure is negative.

Sample size	We assembled the largest possible sample size to maximize the number of novel loci. This approach was effective because we identified many novel loci for intra-ocular pressure and demonstrated that they were relevant to glaucoma.
Data exclusions	Some samples were excluded based on genetic ancestry to ensure homogeneity. This is described in the first two sections of the methods.
Replication	We assembled multiple independent sample sets for both the intraocular and the glaucoma arms of the project.
Randomization	Samples were from collected study cohorts and were not randomized.
Blinding	Genotyping and quality control for the genetic data was conducted without knowledge of the phenotypes.

## Reporting for specific materials, systems and methods

### Materials & experimental systems

n/a	Involved in the study
<input checked="" type="checkbox"/>	<input type="checkbox"/> Unique biological materials
<input checked="" type="checkbox"/>	<input type="checkbox"/> Antibodies
<input checked="" type="checkbox"/>	<input type="checkbox"/> Eukaryotic cell lines
<input checked="" type="checkbox"/>	<input type="checkbox"/> Palaeontology
<input checked="" type="checkbox"/>	<input type="checkbox"/> Animals and other organisms
<input type="checkbox"/>	<input checked="" type="checkbox"/> Human research participants

### Methods

n/a	Involved in the study
<input checked="" type="checkbox"/>	<input type="checkbox"/> ChIP-seq
<input checked="" type="checkbox"/>	<input type="checkbox"/> Flow cytometry
<input checked="" type="checkbox"/>	<input type="checkbox"/> MRI-based neuroimaging

## Human research participants

Policy information about [studies involving human research participants](#)

Population characteristics	Described in full in the methods section.
Recruitment	Described in full in the methods section.